

Fast protein tertiary structure retrieval based on global surface shape similarity

Lee Sael,¹ Bin Li,¹ David La,² Yi Fang,³ Karthik Ramani,³ Raif Rustamov,⁴ and Daisuke Kihara^{1,2,5,6*}

¹ Department of Computer Science, College of Science, Purdue University, West Lafayette, Indiana 47907

² Department of Biological Sciences, College of Science, Purdue University, West Lafayette, Indiana 47907

³ Department of Mechanical Engineering, College of Engineering, Purdue University, West Lafayette, Indiana 47907

⁴ Department of Mathematics, College of Science, Purdue University, West Lafayette, Indiana 47907

⁵ Markey Center for Structural Biology, Purdue University, West Lafayette, Indiana 47907

⁶ The Bindley Bioscience Center, Purdue University, West Lafayette, Indiana 47907

ABSTRACT

Characterization and identification of similar tertiary structure of proteins provides rich information for investigating function and evolution. The importance of structure similarity searches is increasing as structure databases continue to expand, partly due to the structural genomics projects. A crucial drawback of conventional protein structure comparison methods, which compare structures by their main-chain orientation or the spatial arrangement of secondary structure, is that a database search is too slow to be done in real-time. Here we introduce a global surface shape representation by three-dimensional (3D) Zernike descriptors, which represent a protein structure compactly as a series expansion of 3D functions. With this simplified representation, the search speed against a few thousand structures takes less than a minute. To investigate the agreement between surface representation defined by 3D Zernike descriptor and conventional main-chain based representation, a benchmark was performed against a protein classification generated by the combinatorial extension algorithm. Despite the different representation, 3D Zernike descriptor retrieved proteins of the same conformation defined by combinatorial extension in 89.6% of the cases within the top five closest structures. The real-time protein structure search by 3D Zernike descriptor will open up new possibility of large-scale global and local protein surface shape comparison.

Proteins 2008; 72:1259–1273.

© 2008 Wiley-Liss, Inc.

Key words: protein surface shape; protein structure classification; database search; structure similarity; 3D Zernike descriptor.

INTRODUCTION

The three dimensional (3D) structure, especially the surface, plays a central role in various function of proteins. For example, a group of atoms in an active site on the 3D surface of the protein that carries out the catalytic reaction of an enzyme.¹ Further, surface residues on an interface region establish physical contacts to another protein in protein–protein interactions.^{2,3} Therefore, classification of the 3D structure of proteins using an appropriate representation is critical for understanding the universe of protein structure, function, and evolution.⁴

The importance of characterization and comparison of protein 3D structure is further increasing recently in the context of protein function prediction,^{5–7} because a significantly increasing number of structures of unknown function have been solved in recent years by structural genomics projects.^{8–10} Currently, more than 2100 protein structures classified as “unknown function” have been deposited to the Protein Data Bank (PDB),¹¹ whose function are not easily assigned by conventional sequence database search methods.^{12,13} To go beyond sequence data search methods, using the 3D structure information is a reasonable and promising strategy because the evolutionary history could be better traced by using global 3D structures than from sequence alone^{14,15} and local structure similarity search methods could be used to identify catalytic residues involved in the same enzymatic function.^{16–18}

Several different representations have been proposed for comparing protein structures.^{19,20} The most intuitive way would be to compare coordinates of corresponding residues (α carbons in the main chain) or atoms of two proteins. Distance measurement by the root mean square deviation (RMSD) is appropriate when two proteins have the same length and have a similar overall main chain orientation.²¹ When two proteins have different chain lengths, residue correspondence

Grant sponsor: National Institutes of Health (National Institute of General Medical Sciences); Grant numbers: R01 GM075004, U24 GM077905; Grant sponsor: National Science Foundation; Grant number: DMS 0604776.

Lee Sael and Bin Li have equally contributed to this work.

*Correspondence to: Daisuke Kihara, Department of Biological Sciences, Purdue University, West Lafayette, IN 47907. E-mail: dkihara@purdue.edu.

Received 24 August 2007; Revised 15 January 2008; Accepted 11 February 2008

Published online 24 March 2008 in Wiley InterScience (www.interscience.wiley.com).

DOI: 10.1002/prot.22030

needs be predetermined to compute RMSD. That can be done, for example, by combining the RMSD computation by structure superimposition with the dynamic programming (DP) algorithm^{22–24} or an iterative use of DP.²⁵ Also, comparing the distance map of proteins can quantify similarity of proteins based on contacts of residues.^{26,27} A more coarse protein representation uses vectors that describe secondary structure segments and compares spatial arrangements of secondary structures.²⁸

An important point to note is that different protein structure comparison methods compare different features of protein structures. Thus distances of protein structures defined by different methods differ and consequently, database search results by different methods inevitably differ. To illustrate this, consider three programs, Combinatorial Extension (CE),²³ Structure ALignment algorithm (SAL),²² and COmparison of Spatial Arrangements of SECondary structural elements (COSEC).²⁸ CE and SAL can be categorized in the same class of algorithms because both use DP as the basis of their algorithms. However, their behavior is very different: CE first identifies similar fragment pairs of a fixed length between inputs of two protein structures without allowing gaps in fragments, and then extends the combination of similar fragment pairs. On the other hand, SAL uses DP iteratively, allowing gaps in a structural alignment to find statistically significant matches in overall corresponding residues between two proteins. As a result, corresponding protein pairs judged as similar by CE tend to have fragments of the same secondary structure, whereas protein pairs found by SAL often have very different corresponding fragments because it allows gaps in them. Now, CE and COSEC are similar with each other in the sense that both compare ungapped fragments as the basis of structure comparison. However, a large difference exists between them. CE compares fragments of two proteins in a sequential order by DP, whereas COSEC compares spatial arrangement of fragments of two proteins without considering sequential connectivity of fragments. Therefore, CE is more suitable for finding similarity and dissimilarity of relatively closely related proteins, whereas COSEC can find distantly related protein pairs that have circular permutation or domain insertions,²⁹ which CE cannot. SAL is powerful in finding overall fold similarity of proteins that is missed by CE or COSEC. This feature of SAL is especially useful for finding template structures for protein structure prediction.^{22,30} The important thing is to understand strengths and main purposes of each structure comparison algorithm, and use appropriate algorithm for questions one wants to ask.

Here, we use another representation of global structure of proteins that concerns the surface shape of proteins. A surface representation does not consider either of individual residue/atom positions or arrangement of secondary structure segments.³¹ The surface of a protein has been represented in several ways, including tessella-

tion,^{32,33} α -shape,³⁴ and spherical harmonics.³⁵ In this study, we introduce for the first time the 3D Zernike descriptor³⁶ as a representation of the protein surface shape, which is based on a series expansion of a given 3D function.

The reason why we use the 3D Zernike descriptor is because it has several strong advantages. First, compared with conventional methods, it allows fast retrieval of protein structures. The current major structure databases, including PDB, CATH,³⁷ and SCOP³⁸ only allow keyword search and browsing of precomputed classification. The Distance matrix ALignment (DALI) server,³⁹ Vector Alignment Search Tool (VAST) search at National Center for Biotechnology Information (NCBI),⁴⁰ and eF-site database⁴¹ allow users to search the database with a query structure, but a search often takes hours to finish. Ideally, for a routine use of protein structure comparisons against a large number of structures should be done quickly, similar to that of a Basic Local Alignment Search Tool (BLAST) search. Second, 3D Zernike descriptors are rotation invariant, that is, protein structures need not be aligned for comparison. Related works, such as the multipole method⁴² proposed for global protein shape comparison and an application of spherical harmonics for binding pocket and ligand comparisons by Morris *et al.*,⁴³ need pose normalization because the methods are not rotation invariant. The multipole method uses a reference frame that is computed based on the residue C- α coordinates, and the work by Morris *et al.* poses a protein by first, second, and third moments of around the mean of surface positions. Generally speaking, pose normalization could be problematic⁴⁴ especially in comparison of protein shapes, which are almost globular and determining the principle axes may not be robust. Third, the resolution of the description of protein structures can be easily and naturally adjusted by changing the order of 3D Zernike descriptors. For example, the rough global difference of protein structures reflects the difference of the first couple of invariants that correspond to lower orders of the 3D Zernike descriptor. Moreover, other characteristics of a protein surface, such as electrostatic potentials, can be naturally incorporated into the description considering an appropriate 3D function, which will be described elsewhere.

This manuscript is organized as follows: we first describe our implementation of 3D Zernike descriptor for protein surface shape retrieval. Then, differences of the 3D Zernike descriptor and the other projection-based methods are extensively discussed. Next, we report the results of our benchmark on the performance in protein structure search using a large dataset with 2432 proteins. The overall results showed a good agreement with structure comparison by the CE program,²³ which compares main chain orientations of proteins, despite the difference in view of protein shape by the two methods. We also compared 3D Zernike descriptor with another stand-

ard protein structure comparison method, DALI,²⁶ and four other 3D object comparison methods in the computer graphics and engineering domain. Finally, differences between CE and 3D Zernike are shown, emphasizing the advantage of 3D Zernike. The effect of shape comparison at different resolution is also discussed.

METHODS

Building a surface of a protein

The first step of computing 3D Zernike descriptor of a protein is to define the protein surface region in 3D space. To begin with, hetero atoms including water molecules in the PDB file of the target protein are removed. Then, the MSROLL program in Molecular Surface Package version 3.9.3³³ is used to compute the Connolly surface (triangle mesh) of the protein using default parameters. Next, the triangle mesh is placed in a 3D cubic grid of N^3 ($N = 200$), compactly fitting a protein to the grid. Each voxel (a cube defined by the grid) is assigned either 1 or 0; 1 for a surface voxel that locates closer than 1.7 grid interval to any triangle defining the protein surface, and 0 otherwise. Thus, the thickness of the protein surface is 3.4 grid intervals. The inside of a protein is kept empty so that 3D Zernike descriptor focuses on capturing the surface shape of a protein.

3D Zernike descriptor

To obtain 3D Zernike descriptors, one expands a given 3D function $f(x)$ into a series in terms of Zernike-Canterakis basis³⁶ defined by the collection of functions

$$Z_{nl}^m(r, \vartheta, \varphi) = R_{nl}(r)Y_l^m(\vartheta, \varphi) \quad (1)$$

with $-l < m < l$, $0 \leq l \leq n$, and $(n - l)$ even. Here $Y_l^m(\vartheta, \varphi)$ are spherical harmonics.⁴⁵ Spherical harmonics is the angular portion of an orthogonal set of solutions to Laplace's equation, which is given by

$$Y_l^m(\vartheta, \varphi) = N_l^m P_l^m(\cos \vartheta) e^{im\varphi} \quad (2)$$

Here N_l^m is a normalization factor

$$N_l^m = \sqrt{\frac{2l+1}{4\pi} \frac{(l-m)!}{(l+m)!}} \quad (3)$$

And P_l^m is the associated Legendre functions.

$R_{nl}(r)$ are radial functions defined by Canterakis, constructed so that $Z_{nl}^m(r, \vartheta, \varphi)$ are polynomials when written in terms of Cartesian coordinates as follows:

The conversion between spherical coordinates and Cartesian \mathbf{x} is defined as

$$\mathbf{x} = |\mathbf{x}|\zeta = r\zeta = r(\sin \vartheta \sin \varphi, \sin \vartheta \cos \varphi, \cos \vartheta)^T \quad (4)$$

Then the harmonics polynomials e_l^m are defined as

$$e_l^m(\mathbf{x}) \equiv r^l Y_l^m(\vartheta, \varphi) = r^l c_l^m \left(\frac{ix - y}{2} \right)^m z^{l-m} \\ \times \sum_{\mu=0}^{\lfloor \frac{l-m}{2} \rfloor} \binom{l}{\mu} \binom{l-\mu}{m+\mu} \left(-\frac{x^2 + y^2}{4z^2} \right)^\mu \quad (5)$$

where c_l^m are normalization factors:

$$c_l^m = c_l^{-m} = \frac{\sqrt{(2l+1)(l+m)!(l-m)!}}{l!} \quad (6)$$

Using the harmonics polynomials e_l^m , 3D Zernike functions [Eq. (1)] can be rewritten in Cartesian coordinates:

$$Z_{nl}^m(\mathbf{x}) = R_{nl}(r)Y_l^m(\vartheta, \varphi) = \sum_{v=0}^k q_{kl}^v |\mathbf{x}|^{2v} r^l Y_l^m(\vartheta, \varphi) \\ = \sum_{v=0}^k q_{kl}^v |\mathbf{x}|^{2v} e_l^m(\mathbf{x}) \quad (7)$$

where $2k = n - l$ and the coefficient q_{kl}^v are determined as follows to guarantee the orthonormality of the functions within the unit sphere,

$$q_{kl}^v = \frac{(-1)^k}{2^{2k}} \sqrt{\frac{2l+4k+3}{3}} \\ \binom{2k}{k} (-1)^v \frac{\binom{k}{v} \binom{2(k+l+v)+1}{2k}}{\binom{k+l+v}{k}} \quad (8)$$

Now 3D Zernike moments of $f(\mathbf{x})$ are defined as the coefficients of the expansion in this orthonormal basis, that is, by the formula

$$\Omega_{nl}^m = \frac{3}{4\pi} \int_{|\mathbf{x}| \leq 1} f(\mathbf{x}) \bar{Z}_{nl}^m(\mathbf{x}) d\mathbf{x}. \quad (9)$$

To achieve rotation invariance, the moments are collected into $(2l + 1)$ dimensional vectors $\Omega_{nl} = (\Omega_{nl}^l, \Omega_{nl}^{l-1}, \Omega_{nl}^{l-2}, \Omega_{nl}^{l-3}, \dots, \Omega_{nl}^{-l})$ and define the rotationally invariant 3D Zernike descriptors F_{nl} as norms of vectors Ω_{nl} . Thus

$$F_{nl} = \sqrt{\sum_{m=-l}^{m=l} (\Omega_{nl}^m)^2} \quad (10)$$

Index n is called the order of the descriptor. The rotational invariance of 3D Zernike descriptors means that calculating F_{nl} for a protein and its rotated version would yield the same result.

In this work, binary voxelization of a protein structure is used, that is, function $f(\mathbf{x})$ is defined to be 1 at the points sufficiently close (within about one voxel size) to the surface of the protein, and 0 at all other locations. The order n determines the resolution of the descriptor. It was shown in a previous study that the order of $n = 20$ (i.e., a total of 121 numbers to index each shape) provides sufficient accuracy.³⁶

Definition of distance used in this study

Now that a protein 3D structure is represented by 121 numbers, a comparison of two protein 3D structures simply results in a comparison of two series of the 121 numbers. In this study, we used three distance measures for comparing 3D Zernike descriptor of protein surface shapes. The first function is the Euclidean distance, d_E , which is the RMSD of corresponding index numbers of two proteins:

$$d_E = \sqrt{\sum_{i=0}^{i=nl} (z_{Ai} - z_{Bi})^2} \quad (11)$$

where Z_{Ai} is the i th number of 3D Zernike descriptor of protein A, n is the order of descriptor, and $0 \leq l \leq n$, and $(n - l)$ even as described earlier.

The second function is the Manhattan distance, d_M , which is the sum of the difference of each corresponding index numbers:

$$d_M = \sum_{i=0}^{i=nl} |z_{Ai} - z_{Bi}| \quad (12)$$

The third distance, d_C , is defined as

$$d_C = 1 - \text{Correlation Coefficient} (Z_A, Z_B) \quad (13)$$

Thus $d_C = 0$ when two descriptors correlates perfectly.

3D Zernike descriptor and spherical harmonic descriptor

In this section, we discuss 3D Zernike descriptors mainly in comparison with the spherical harmonics descriptors (SHD),^{46,47} which is a popular spherical harmonics-based projection techniques used for general 3D object comparison. Projection-based techniques have been used extensively in two-dimensional (2D) image analysis and pattern recognition.^{48–52} In particular, 2D Zernike moments have proved exceptionally useful for the analysis of 2D shapes arising in many areas ranging from face recognition,⁵³ cell parts recognition,⁵⁴ and optical scattering pattern recognition for identifying bacterial colonies.⁵⁵ Yeh *et al.*⁵⁶ applied 2D Zernike moments to protein 3D structure retrieval by characterizing a structure with a set of 2D projections from 100 different directions. Finally, Canterakis was able to extend 2D Zernike polynomials and moments to 3D, introducing 3D

Zernike-Canterakis polynomials.⁵⁷ Later, rotationally invariant descriptors based on Zernike-Canterakis moments were explored for 3D shape retrieval by Novotni and Klein,³⁶ who reported improved precision-recall curves at a lower storage cost when compared with SHD.

For SHD no radial modulation is used; rather, the 3D space is sampled into concentric spherical shells around the center of mass. Then, a volume of a target object within each concentric sphere of a radius r centering at the center of mass of the object, $f_r(\vartheta, \varphi)$, is expanded in the series of spherical harmonics, $Y_l^m(\vartheta, \varphi)$:

$$f_r(\vartheta, \varphi) = \sum_l f_r^l(\vartheta, \varphi) = \sum_l \sum_{m=-l}^l c_{r,l}^m Y_{r,l}^m(\vartheta, \varphi) \quad (14)$$

Spherical harmonics differs under different orientations, (ϑ, φ) . However, since the L_2 norm of the function is rotation invariant, a rotation invariant signature for $f_r(\vartheta, \varphi)$ is constructed as the collection of L_2 norms of $f_r^l(\vartheta, \varphi)$ at each l , that is, $\{\|f_r^0\|, \|f_r^1\|, \dots\}$. Finally, collecting the signature for each radius, r , will give the SHD of a protein structure. The implementation uses 32 shells, 17 descriptors per shell, making a total of 544 numbers to represent a shape.

Let us remark that 3D Zernike descriptors genuinely belong to the 3D realm, while SHD are essentially a combination of 2D descriptors. Indeed, note that SHD measures similarity of objects by comparing them shell-wise. There are quite a few practical implications of this fact: (1) SHD does not capture object coherence in the radial direction, thereby incorporating less object characteristic information.³⁶ For example, since the descriptors for each shell are calculated separately, the shells can be rotated independently by random angles without changing the resulting descriptors. (2) The orthonormality of the Zernike-Canterakis basis results in less information redundancy. One should note that in SHD, descriptors coming from adjacent shells are highly correlated, making them redundant to some extent. Indeed, using 154 3D Zernike descriptors (max order 21) yields better retrieval results than using 928 SHDs (32 shells, 29 descriptors per shell) as tested on the Princeton Shape Benchmark, which is a database of general 3D objects such as airplanes and chairs.^{36,47} (3) SHDs require polar sampling, which was pointed out to be problematic for the robustness of rotation invariancy.⁵⁸ Securing robustness of SHD requires a distance field-based voxelization procedure where voxels are assigned continuous values between 0 and 1. On the other hand, the Zernike-Canterakis basis consists entirely of polynomials in Cartesian coordinates, thus avoiding polar sampling, and making possible to treat all voxels in the model on equal footing. In addition, 3D Zernike descriptors show optimal performance when simple binary voxelization is used.³⁶

Because sizeable amount of the computational time is consumed by the voxelization process, this simplicity results in faster response times for user-search engine transactions. (4) One can naturally add other protein surface properties within the 3D Zernike framework. For example, to add electrostatics, it is enough to calculate 3D Zernike descriptors of $f(x)$ set equal to the electrostatic potential value on the surface, and zero otherwise. This is not as straightforward with the SHD, because of the aforementioned robustness problem.

Comparison with the other surface shape-based structure representation methods

The 3D Zernike descriptor is compared with four other methods in terms of the performance on retrieving similar protein structures. The benchmark dataset used is described in the next section. The all four methods represent surface shape of objects, namely, the SHD,^{47,46} the solid angle histogram (SAH),^{59,60} the shape distribution,⁶¹ and the eigen value model.⁶⁰ These methods have been developed and used for recognition of 3D shapes in computer graphics and engineering domain. Below we briefly describe the idea of these methods.

To compute aforementioned SHD of a protein structure, first the protein structure is voxelized. We used the SpharmonicKit package (<http://www.cs.dartmouth.edu/~geelong/sphere/>) for computing SHD. The Euclidean distance was used to compare SHDs of two proteins.

The SAH represents a distribution of local concavity and convexity of a protein structure. To obtain SAH, a protein is first voxelized. Let $K_{c,r}$ denote a set of voxels included in a sphere of a radius of r with the center at a voxel c . Then, the solid angle value $SA(v_i, r)$ at a voxel v_i for a protein volume V is defined as the fraction of the intersection volume of a sphere $K_{v_i,r}$ with the protein volume V relative to the volume of the sphere $K_{v_i,r}$:

$$SA(v_i, r) = \frac{|K_{v_i,r} \cap V|}{|K_{v_i,r}|} \quad (15)$$

Hence, a histogram of $SA(v_i, r)$ represents a protein structure. The SAHs of two proteins are compared by the L_1 norm as suggested in the previous work.⁶⁰

The shape distribution method describes an object as a histogram of the length of pairs of points on the surface of the object. First, a given protein is voxelized and the distance distribution is computed by randomly sampled pairs of voxels on the protein surface. We use L_2 norm to compute the distance of voxel pairs and L_1 norm to compare the similarity of two shape distributions.

The eigen value model⁶⁰ represents a given protein as a set of eigen values. The model first voxelize the protein into a 3D grid and divides the grid into cells. Then for each cell, three eigen values of the distribution of the points (voxels) are computed, resulting in total of $3p^3$

eigen values. These eigen values are registered in the according bins of a histogram, which describes the protein structure. Two histograms are compared by L_1 norm.

In a comparative study of performance of earlier methods on retrieval of engineering parts (e.g., bolts, wheels),⁶² it was shown that their performance varies depending on parts. Therefore, it was our curiosity that whether these methods originally developed for general objects and engineering parts can be used for protein structure search or not.

Benchmark dataset

The benchmark dataset of protein structures consists of 2432 protein structures classified into 185-fold groups. These are a subset of structures extracted from a structure comparison results by the CE program²³ (ftp://ftp.sdsc.edu/pub/sdsc/biology/CE/db/ata_3_8.txt). Note that the structure representation of CE and 3D Zernike descriptor is fundamentally different: the former consider a protein structure as the spatial position of main-chain residues and the latter represents a protein structure as a surface shape. The purpose of this benchmark study is to investigate the extent of similarity between the two methods. If we observe a significant agreement between the two methods, which result suggests that 3D Zernike descriptor can be an effective tool for fast search of protein structures with a similar main-chain orientation (i.e., a conventional sense of protein structure similarity, which also implies evolutionary relationship) not only a similar surface shape. On the other hand, it is also expected that interesting cases that two proteins that share a similar surface shape but different main-chain orientation can be found. CE is one of the standard programs for protein main-chain comparison that classifies proteins solely by geometrical aspect of proteins without consideration of evolutionary relationship as, for example, SCOP database does. Given two protein structures, CE first identifies eight residue-long fragments of a similar conformation in the two proteins by comparing corresponding distances of pair of residues within each fragment. Then, identified fragment pairs from the two proteins are combined to find larger structurally similar regions by comparing corresponding interfragment distances. DP is used for the calculation, thus fragment pairs are combined in a sequential order from the N-terminus to the C-terminus. Below describes the procedure we used to select the benchmark proteins.

The original CE database consists of 50,246 protein structures classified into 7386-fold groups. Each fold group consists of a “representing” protein, a set of “represented” proteins that satisfy several similarity criteria against the representing protein, and another set of “similar” proteins (see the README file of the database for more technical details). Starting from the CE database, first, separate fold groups are merged if the structure of

their “representing” proteins is sufficiently similar, having a *Z*-score of 3.8 or higher by CE. The *Z*-score of 3.8 is recommended by the authors of the database to filter out random similarities. Next, the set of “similar” proteins are eliminated from a fold group. Then, “represented” proteins are eliminated from a fold group if the size is more than 12.5% different in length from the “representing” protein, or if the quality of the structure is not appropriate: structures that lack coordinates of more than 10 residues, or which have only coordinates of α carbons, are removed. Small proteins that have less than 100 residues are also eliminated. In addition, structures that have coordinates of hydrogen atoms of more than 3% of residues are filtered out, because they significantly affect surface shape of the protein. Finally, small groups that only contain three or less “represented” proteins (and “representing” protein) are removed.

DALI protein structure comparison program

In addition, we also run the DALI algorithm²⁶ against the CE based benchmark dataset. DALI is another widely used protein structure comparison algorithm that is established in 1993. DALI compares two protein structures in terms of the 2D distance map of the proteins. First, DALI identifies similar subdistance maps of two input proteins of a fixed size by comparing corresponding distances between two subdistance maps. This step captures local regions of the two proteins that have a similar residue contact pattern. Next, the algorithm combines identified pairs of similar subdistance maps to find significantly similar structures between the two proteins. We used the standalone program of the DALI algorithm, DaliLite,⁶³ which is available for download at <http://www.ebi.ac.uk/DaliLite/>.

Benchmark procedure

For each protein, the whole set of proteins are ranked by a given distance of the 3D Zernike descriptor. For a given distance threshold value, the sensitivity and the specificity are averaged within a group, then again averaged among all groups to give a final value in the plots (see Fig. 3). The sensitivity and the specificity are defined as follows:

$$\text{Sensitivity} = \frac{TP}{TP + FN} \quad (16)$$

$$\text{Specificity} = \frac{TP}{TP + FP} \quad (17)$$

where TP, true positive, is the number of fold group members of a query protein retrieved with a distance closer than the threshold; FN, false negative, is the number of the fold group members whose distance to a query

protein is larger than the threshold hence missed in the search; FP, false positive, is the number of proteins that are not included in the fold group with the query protein but incorrectly retrieved in the search. Thus, the denominator in Eq. (16) is the total number of all members of the fold group. The denominator in Eq. (17) is the total number of proteins retrieved above the threshold.

RESULTS

Examples of 3D Zernike descriptor

Figure 1 shows examples of 3D Zernike descriptor of two proteins, triosephosphate isomerase (PDB code: 7tim, A chain) and interleukin-4 receptor α -chain (1iarB). Globally, 7timA has more or less a round-shaped surface and 1iarB is an L-shaped structure [Fig. 1(A)]. This apparent difference of their global surface shape is reflected by distinctive 3D Zernike descriptors shown in Figure 1(B). The difference in the overall shape tends to appear in the first couple of orders of the descriptor,

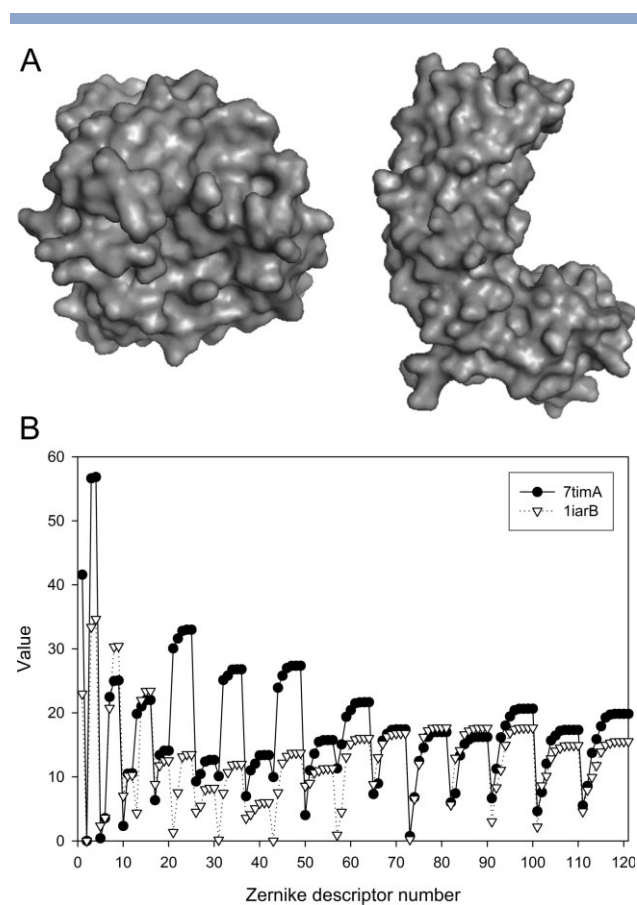


Figure 1

3D Zernike descriptor of two example proteins. A, The global surface shape of the two proteins; 7timA (left) and 1iarB (right). B, 3D Zernike descriptor of the two proteins. Circles, 7timA; and triangles, 1iarB.

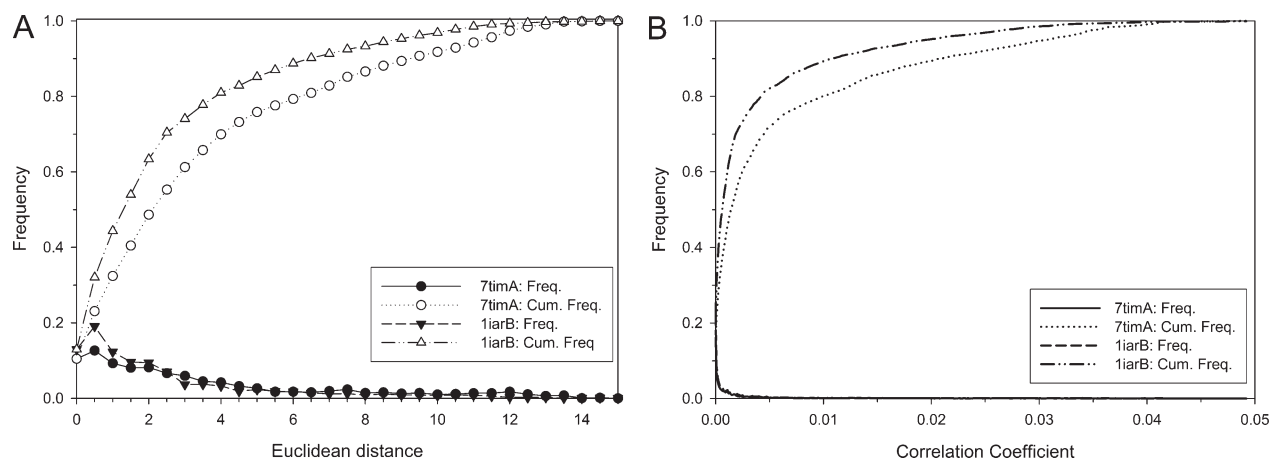


Figure 2

Variance of 3D Zernike descriptor upon rotation of proteins. All the possible rotated positions of two protein structures, 7timA and 1iarB, in three orthogonal directions with a step size of 30° are computed. Histograms of distances of 3D Zernike descriptor between each of the rotated structures and the original one are shown. **A**, The Euclidean distance is used. Filled (empty) circles, the frequency (the cumulative frequency) of Euclidean distances of 7timA are plotted. Filled (empty) triangles, the frequency (the cumulative frequency) of Euclidean distances of 1iarB are plotted. **B**, The correlation coefficient based distance is used. The frequency and the cumulative frequency of distances of 7timA and 1iarB are shown by solid line, dotted line, dashed line, dash-dot-dot line, respectively.

resulting in a relatively large Euclidean distance of 38.84, and correlation coefficient-based distance of 0.656.

Rotation invariance

As described earlier and in Method section, the 3D Zernike descriptor is mathematically most noteworthy rotationally invariant. This is one of the largest advantages of 3D Zernike descriptor. However, in practice the descriptor of rotated protein structures are not exactly identical. This error is caused possibly when the protein surface shape is discretized into voxels. We found that in computing all the distance measures, that is, Euclidean [Eq. (11)], Manhattan [Eq. (12)], and the correlation coefficient-based [Eq. (13)], normalizing each number in a 3D Zernike descriptor by the sum of the 121 numbers of the descriptor reduces the error the best among tested methods. Figure 2 shows an example of the variance of 3D Zernike descriptor upon rotation. Here, the two proteins used in Figure 1 are rotated to all the possible positions, and Euclidean and the correlation coefficient-based distance from the original position are computed. We used these two distances because they were the top two performing functions in our protein shape search benchmark (see the next section). As for Euclidean distance [Fig. 2(A)], approximately 90% of the rotated structures stay within the distance of 10. In the case of the correlation coefficient-based distance [Fig. 2(B)], approximately 90% of the rotated structures of the two proteins have less than a distance of 0.03. From this experiment, we can draw a threshold of the significance of the distance, or in the other words, determine an “invisible” range of

the 3D Zernike descriptor. For example, if two proteins have an Euclidean distance of less than 10, these proteins can be considered significantly similar, or more precisely, indistinguishable from the case where the two proteins are identical but placed in a different orientation.

To improve the rotation invariance of the descriptor, we have tried different thickness of the surface representation, and also a continuous value assignment between 0 and 1 to surface voxels rather than the binary voxelization, but did not observe differences in the performance.

Structure retrieval by three different methods

One of the most interesting applications of 3D Zernike descriptor is fast structure retrieval. In this experiment, we used a database derived from the CE algorithm²³ to define the structure similarity. It is important to note that the structure similarity depends on how structures are represented and compared.^{19,64} CE uses combination of similar main chain fragments to compute the similarity of two protein structures. On the other hand, 3D Zernike descriptor compares surface shape and DALI compares the distance maps of two proteins.

Let us first compare the CE benchmark dataset with the SCOP protein classification database³⁸ to understand the nature of protein structure classification. The unique feature of SCOP is that evolutionary relationship of proteins is also taken into account by manual curation together with protein structure similarity. Thus SCOP has been serving as an indispensable resource for elucidating relationships of protein structure and function.

Table I*Comparison Between the CE Based Benchmark Dataset and the SCOP Database*

Overlap ^a	The number of CE groups (%) ^b
(A) Comparison with the superfamily classification by SCOP	
0–0.1	1 (0.5)
0.1–0.2	0
0.2–0.3	0
0.3–0.4	1 (0.5)
0.4–0.5	5 (2.7)
0.5–0.6	15 (8.1)
0.6–0.7	5 (2.7)
0.7–0.8	7 (3.8)
0.8–0.9	11 (5.9)
0.9–1.0	2 (1.1)
1.0	139 (75.1)
(B) Comparison with the fold classification by SCOP	
0–0.1	1 (0.5)
0.1–0.2	0
0.2–0.3	0
0.3–0.4	0
0.4–0.5	1 (0.5)
0.5–0.6	10 (5.4)
0.6–0.7	4 (2.2)
0.7–0.8	8 (4.3)
0.8–0.9	8 (4.3)
0.9–1.0	2 (1.1)
1.0	152 (82.2)

^aThe fraction of members of a fold group in the CE-based benchmark dataset that overlap with a superfamily in SCOP. When a CE-fold group corresponds to multiple SCOP superfamilies, a SCOP superfamily that gives the largest overlap with the CE fold group is used to compute the fraction.

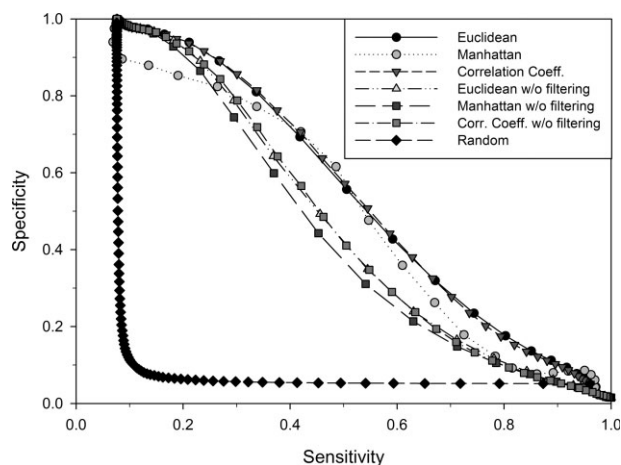
^bThe percentage among the 185 CE-fold groups.

In Table I(A), the 185-fold groups in the CE benchmark dataset are compared with the superfamilies defined in SCOP. The number of CE-fold groups that overlap with a SCOP superfamily by a certain fraction is counted. When a CE-fold group overlaps with several SCOP superfamilies, the SCOP superfamily that gives the largest overlap is counted. The number of SCOP superfamilies that correspond to the CE benchmark dataset is 150, which is smaller than the number of the CE-fold groups. It is found that only 75.1% of the CE-fold groups correspond to one SCOP superfamily. Table I(B) shows that 82.2% of the CE-fold groups correspond to one SCOP fold. The overlap with SCOP folds looks larger than SCOP superfamilies, because the average size of SCOP fold is larger, thus it is more frequent that multiple CE-fold groups correspond to a SCOP fold. The number of SCOP folds that correspond to the CE benchmark is 117. These results illustrate that even the widely used protein structure comparison method, CE, does not have perfect correspondence with a well-established protein structure classification database, SCOP. Especially, this implies that CE should be used with caution if the purpose of using CE is to investigate biological function of proteins, because only 75.1% of the CE groups agree with SCOP superfamilies. A recent work by Sierk and Pearson⁶⁵ provides a further benchmark for protein structure comparison

methods. Therefore, the aim of the structure retrieval performed in this study using 3D Zernike descriptor and DALI on the CE benchmark dataset was to understand the similarity and dissimilarity of the three methods, not evaluating “accuracy” of a particular method.

Figure 3 shows the sensitivity and specificity plot of the benchmark performance on a dataset of 2432 proteins. Results of the 3D Zernike descriptor with and without prescreening by the length of the proteins are also shown. When the prescreening is used, a protein in the dataset is compared with a query protein only when its length is in the range of 57%–175% of that of the query protein. The three different distance measures, namely, Euclidian, Manhattan, and the correlation coefficient-based [Eqs. (11)–(13)] are compared. First, regardless of the prescreening, the results are far better than random. Second, among the three distance measures, the performance of Manhattan distance is somewhat worse than the other two distance measures, but all three distance measures essentially showed similar performance. Third, it is shown that the prescreening is effective in improving the search performance. This is because the scale is normalized so that a structure fits in a unit sphere when computing 3D Zernike descriptor, hence the size information is lost.³⁶

Table II summarizes the search results of 3D Zernike descriptor with the length-based prescreening is used. More than 89.0% of proteins retrieved another protein in the same CE-fold group within the top five closest

**Figure 3**

The sensitivity and the specificity of the benchmark dataset are plotted using three distance definitions of 3D Zernike descriptor. The Euclidean (black circles/upward triangles), the Manhattan (gray circles/dark gray squares), and the correlation coefficient-based distance (downward triangles/light gray squares) with and without prescreening by the sequence length. When the prescreening is used, a protein in the dataset is compared with a query only when its length is in the range of 57%–175% of that of the query protein. For comparison, results of a random retrieval are also plotted (black diamonds).

Table II
Summary of the Structure Retrieval Using Different Distance Metrics

	Top 1			Top 5			Top 10			Average rank ^d			Average distance		
	Proteins ^a	Groups 1 ^b	Groups All ^c	Proteins	Groups 1	Groups All	Proteins	Groups 1	Groups All	Proteins	Groups ^e	Proteins	Groups	Proteins	Groups
Euclidean	1881 (77.3)	178 (96.2)	48 (25.9)	2179 (89.6)	182 (98.4)	72 (38.9)	2264 (93.1)	184 (99.5)	91 (49.2)	6.19	9.79	8.31	9.29	71.92	80.04
Manhattan	1846 (75.9)	177 (95.7)	41 (22.2)	2165 (89.0)	181 (97.8)	70 (37.8)	2257 (92.8)	183 (98.9)	88 (47.6)	6.33	10.07	71.92	80.04	71.92	80.04
Correlation coefficient	1873 (77.0)	179 (96.8)	45 (24.3)	2176 (89.5)	183 (98.9)	71 (38.4)	2265 (93.1)	183 (98.9)	92 (49.7)	6.82	10.79	0.02	0.02	0.02	0.02
DaliLite ^f	307 (12.6)	49 (2.0)	0 (0.0)	696 (28.6)	85 (3.5)	1 (0.0)	897 (36.9)	104 (4.3)	1 (0.0)	108.22	183.07	19.90	24.86	19.90	24.86
Random ^g	117 (4.8)	36 (19.5)	0 (0.0)	508 (20.9)	89 (48.1)	0 (0.0)	806 (33.1)	122 (65.9)	1 (5.4)	54.2	87.17	0.09	0.14	0.09	0.14

^aThe number of query proteins that retrieved a correct member in the same group as the first position, within Top 5 or Top 10. In the parentheses, the percentage among all the 2432 proteins in the benchmark set is shown.
^bA group is counted if at least one member in the group successfully retrieved another member in the group as the first position, within Top 5, or Top 10. In the parentheses, the percentage among all the 185 groups in the benchmark set is shown.

^cA group is counted only if all the members in the group successfully retrieved another member in the group as the first position, within Top 5 or Top 10.
^dThe average rank and distance of the closest structure judged by the distance metric to the query.

^eThe rank of proteins is first averaged within a group, then averaged across the groups.

^fDaliLite Version 2.4.4 was used. The distance d is defined as $d = 100 -$ (the structure similarity Z-score by DaliLite).

^gA random value between 0 and 1 is assigned as the distance between the query to each protein.

structures. Those successful proteins are not biased to specific types of protein folds, because the successful proteins are distributed among approximately 98% of the fold groups (Top 5, Group 1). When Top 10 hits are considered, 93.1% of the proteins successfully retrieved its CE-fold group member by using the Euclidean or the correlation coefficient-based distance. The search was successful for at least one protein in almost all the fold groups (99.5% by using the Euclidean distance) considering Top 10 hits. On the other hand, approximately half of the fold groups contain some members that could not retrieve its fold group member within Top 10 (Top 10, Groups All). These are protein structures that are judged to be similar by the main-chain orientation but not by the surface shape. Below in Figure 5, we show examples of these cases.

The structure retrieval results by DaliLite are also shown in Table II. Interestingly, only 28.6% of proteins retrieved another protein in the same CE-fold group within Top 5 by using DaliLite. Actually, the Top 5 and Top 10 results by DaliLite are only slightly better than the random retrieval.

To conclude, overall 3D Zernike descriptor showed a strong agreement in the protein structure retrieval with CE despite its completely different representation of protein structures. 3D Zernike descriptor agrees with CE much more than DALI (i.e., the DaliLite program) does with CE. The superiority of the 3D Zernike descriptor will be clearer when its performance is compared with the other shape comparison methods in Figure 4.

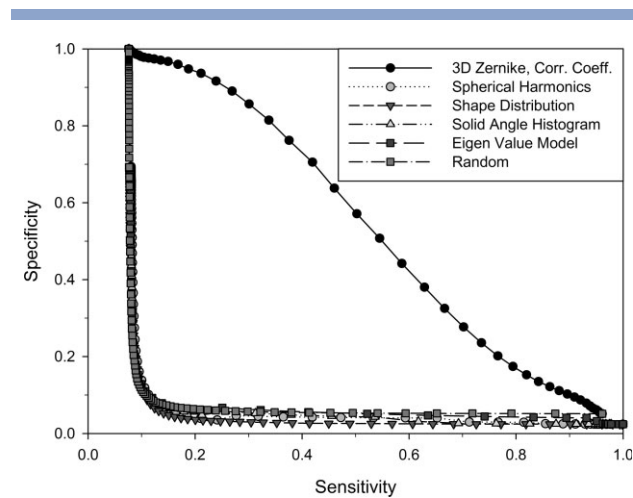


Figure 4

The performance of the 3D Zernike descriptor with the correlation coefficient-based distance (black solid circles) was compared with four other existing shape descriptors, the spherical harmonics descriptor (gray circles), the shape distribution histogram (black triangles), the solid angle histogram (gray triangles), and the eigen value model (black squares). See text for details of these methods. For comparison, the random retrieval is also added (gray squares).

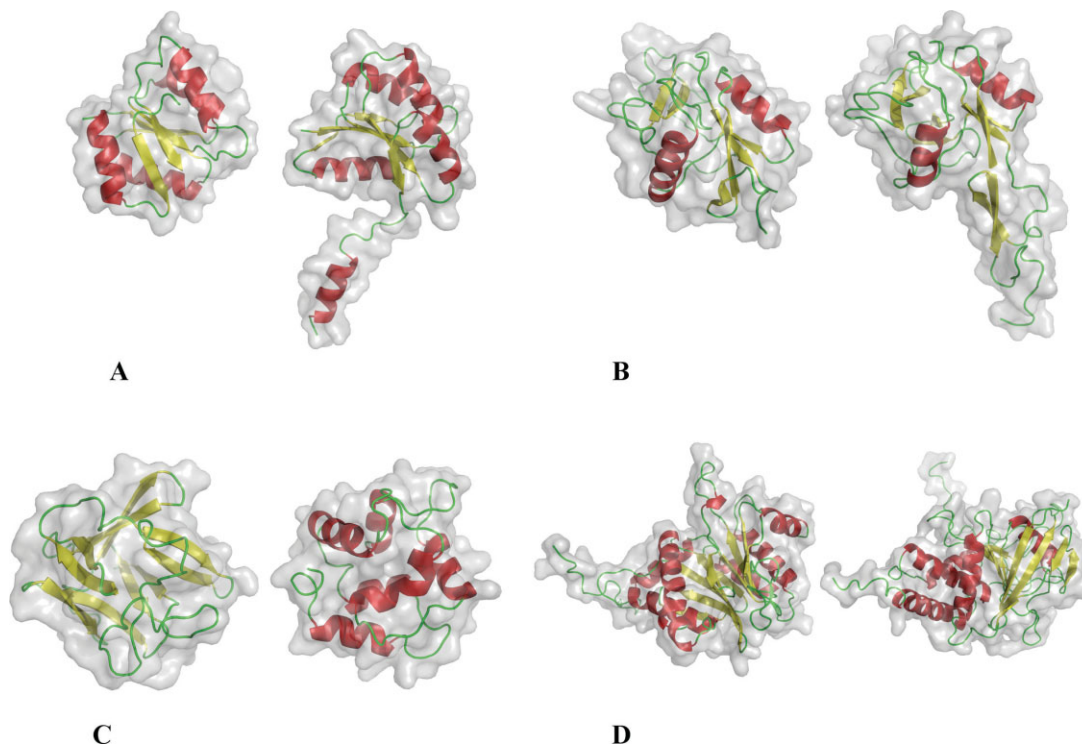


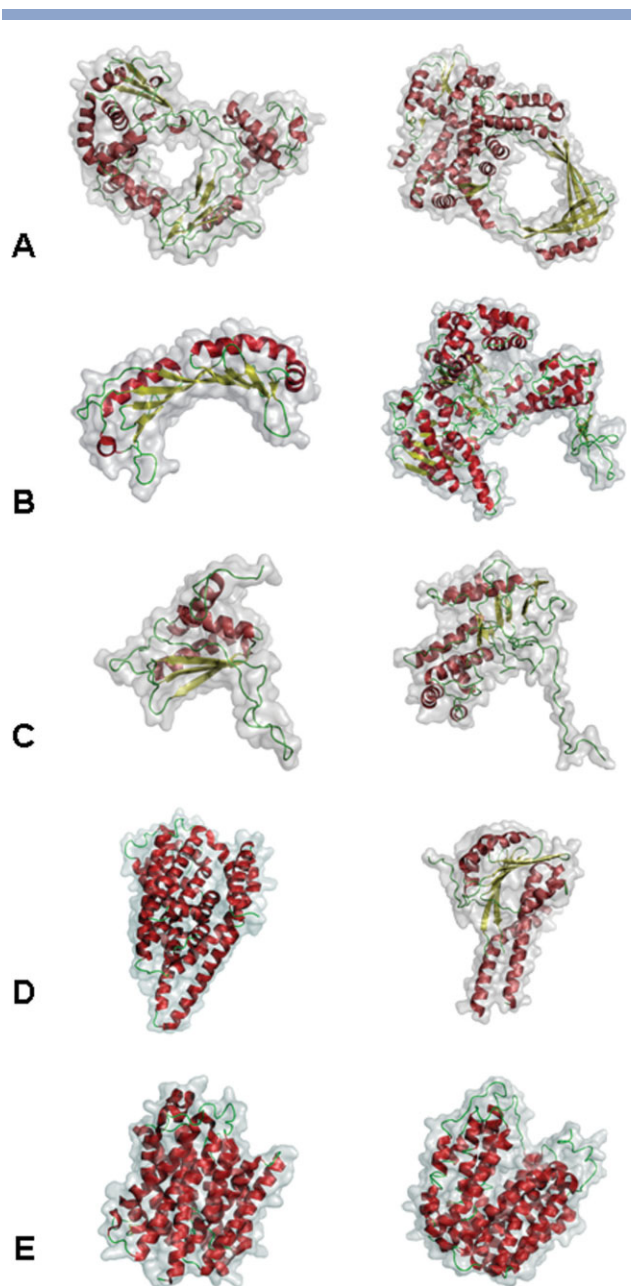
Figure 5

Examples of protein pairs of the same main chain orientation (A, B), and pairs with a similar surface shape but with a different main chain orientation (C, D) are shown. Structural comparisons are performed by CE and 3D Zernike. The comparison between A, 1dz3A (response regulator SPO0A) and 1mb0A (response regulator DIVK). CE computes: RMSD = 1.6 Å, Z-score = 5.0, aligned/gap positions = 104/3, Sequence identity (SeqID) = 26.9%. 3D Zernike shows: Euclidean distance (d_E) = 51.21, Manhattan distance (d_M) = 438.53, correlation coefficient (d_C) = 0.620. B, 1jznA (galactose-specific C-type lectin) and 1g1qA (P-selectin lectin). CE: RMSD = 2.0 Å, Z-score = 5.9, aligned/gap positions = 115/12, SeqID = 23.5%. 3D Zernike: d_E = 52.67, d_M = 431.16, d_C = 0.602. In contrast, C and D demonstrate two instances in which 3D Zernike detect similar global surface shape of proteins with a different overall fold. C, 1barA (fibroblast growth factor) and 1rro (oncomodulin). CE: RMSD = 6.7 Å, Z-score = 1.6, aligned/gap positions = 56/50, SeqID = 3.6%. 3D Zernike: d_E = 12.66, d_M = 101.85, d_C = 0.031. D, 1ryyB (proteasome subunit) and 1gwz (Tyrosine phosphatase). CE: RMSD = 5.0 Å, Z-score = 2.3, aligned/gap positions = 72/70, SeqID = 9.7%, 3D Zernike: d_E = 12.73, d_M = 108.89, d_C = 0.041.

Next, the 3D Zernike descriptor using the correlation coefficient-based distance was compared with four existing shape comparison methods, namely, the SHD, the shape distribution histogram, the SAH, and the eigen value model (see Fig. 4). To our surprise, all these four methods' performance was no better than the random retrieval. This may be due to the protein surface shape being more or less globular, hence all the proteins in the benchmark dataset looked almost the same to the four shape comparison methods developed in computer graphics and engineering domain. The strikingly poor performance of the four methods in Figure 4 reminds us that these methods are originally designed to differentiate general objects, for example, airplanes from cars, trees from chairs, or steering wheels from car doors. In contrast, Figure 4 clearly highlights the appropriateness of 3D Zernike descriptor's utility in the protein shape search, which was revealed to be challenging for conventional shape retrieval methods developed in computer graphics and engineering domain.

Figure 5 illustrates difference between CE and 3D Zernike descriptor. Figure 5(A,B) are protein structure pairs that are identified to be significantly similar by CE, but not by 3D Zernike. They are evolutionary closely related and thus classified into the same family in CATH and SCOP. In these two examples, a small portion of the secondary structure elements of the protein is flipped out (figure on the right) from the mass of the protein, resulting in the change of the surface shape. Figure 5(C,D) are opposite examples. Figure 5(C) is a vivid example of two proteins that have a very similar surface shape but with completely different secondary structure elements, where the left structure is a β class protein and the right structure is an α class protein. Figure 5(D) is a protein pair with a different topology (in CATH) forming a very similar surface shape.

Taking advantage of the 3D Zernike descriptor's ability to find proteins with similar overall protein surface shape, functionally related proteins can be retrieved beyond sequence similarity and significant backbone

**Figure 6**

Examples of protein pairs whose surface shapes are judged to be similar by 3D Zernike descriptor. Detailed data are shown in Table III. A, 1a31 and 1cy0 (from left to right); B, 1tbp and 1t7p; C, 1b3t and 1adv; D, 2nwl and 2bbh; E, 2b2i and 2cfp. Detailed data of these protein pairs are shown in Table III.

conformation similarity. Figure 6 shows several such examples. Associated Table III gives detailed data for the proteins in Figure 6. Figure 6(A) is a pair of DNA topoisomerase I from human and *Escherichia coli*. The characteristic pore of the proteins is to capture DNA double strands. The sequence identity between the two proteins is very low, and the CE only aligns 17.3% of the whole region of the two proteins. In contrast, 3D Zernike

Table III
Pairs of Proteins that have Similar Surface Shape Defined by 3D Zernike Descriptor

PDB ID	Function		SCOP classification		Length (aa)		CE		3D Zernike ^b		
	A	B	A	B	A	B	Z-score	Aligned region (%) ^c	d _E	d _M	d _C
1a31	DNA topoisomerase I (human)	DNA topoisomerase I (<i>E. coli</i>)	d.163.1.2	e.10.1.1	457	534	3.9	79 (17.3)	5.58	49.9	0.001
1tbp	TATA-binding protein	DNA polymerase	d.129.1.1	e.8.1.1	180	662	4.4	64 (35.6)	7.25	58.6	0.08
1b3t	Nuclear DNA binding protein EBNA1	Adenovirus DNA binding protein	d.58.8.1	g.51.1.1	147	287	1.6	64 (43.5)	7.65	69.4	0.28
2nwl	Glutamate transporter	CorA Mg ²⁺ transporter	N/A ^d	d.328.1.1	422	244	2.3	88 (36.1)	6.04	53.6	0.001
2b2i	Ammonium transporter	Lactose permease	N/A	f.38.1.2	399	417	4.4	102 (25.6)	7.28	58.6	0.08

^aThe sequence identity between the two proteins.

^bThe Euclidian (d_E), the Manhattan (d_M), and the correlation coefficient-based (d_C) distance of the 3D Zernike descriptor.

^cThe percentage of the aligned residues relative to the shorter protein among the two.

^dNot included in the current SCOP (ver. 1.73).

Table IV
Execution Time (in s)

Grid size ^a	64 ³ (voxels)	200 ³ (voxels)
Surface triangulation ^b	21	21
Surface voxelization	1	3
3D Zernike descriptor transformation	1	16
Database search ^c	0.43	0.46
Total	24 (s)	41 (s)

^aThe number of voxels where a protein structure is placed.

^bMSROLL program in Molecular Surface Package (ver. 3.9.3) is used.

^cThe benchmark dataset of 2432 proteins used in the current study is searched.

descriptor identifies the overall similar surface shape with a significant distance (compare the 3D Zernike distances with the average distance of the top hit in the benchmark, the right columns in Table II). Figure 6(B) shows two DNA binding proteins. Both proteins bind to DNA with the curved U-shaped region. These two proteins have different function, but both have the characteristic surface shape that enables binding to DNA, that is captured by 3D Zernike descriptor. Figure 6(C) is another pair of proteins. These two proteins bind to DNA with their long tail regions. Note that SCOP classifications of these three pairs are also different from each other. Figure 6(D) is a pair of subunits of membrane protein complexes. 2nwl is a subunit of glutamate transporter, which is a pentamer, and 2bbh is a subunit of CorA Mg²⁺ transporter, which is a trimer. In both the cases, the two long helices penetrate membrane and form the scaffold of the transporters. The last example, Figure 6(E) is a pair of transmembrane proteins. In all the cases [Fig. 6(A–E)], the sequence identity between the pair is below 10%, and CE only aligns partial regions of the pair. In contrast, 3D Zernike descriptor captures overall surface similarity of each pair that is required to realize their biological function with significantly close distance.

Search speed by 3D Zernike descriptor

The 3D Zernike descriptor allows rapid real-time search on the web, because a protein structure is compactly represented by 121 numbers (when the order $n = 20$). If a query protein is already transformed into 3D Zernike descriptor, a search to the current benchmark dataset takes less than a second on an Intel Pentium 4 3.0 GHz processor with 2 GB of memory (Table IV). When a custom PDB file is input as the query, the following steps must be performed before database search: (1) Solvent accessible surface triangulation by Molecular Surface Package,³³ (2) Surface voxelization, and (3) transformation into 3D Zernike descriptor. Taken together with the database search, this entire process takes still less than a minute. Because enlarging the database to be searched only affect the execution time of the database search step, a search against the entire PDB (as of August

2007) with 45,000 structures will only take a minute. The search speed can further be made faster if the database is prescreened by the length of the query protein. Note that a pairwise structure comparison by CE takes typically a couple of seconds. Thus, a database search against PDB using CE would take more than a day.

Structure database searches using 3D Zernike descriptor can be performed through the web at: <http://dragon.bio.purdue.edu/3d-surfer/>. Users can search the benchmark dataset with one of the structures in the dataset (i.e., 3D Zernike descriptor of the protein is precomputed) or by uploading a custom PDB file to the server.

Resolution of the descriptors

As described earlier, one of the characteristics of the 3D Zernike descriptor is that the resolution of the description of shapes can be altered by changing the order of 3D Zernike descriptors. In Figure 7, two different orders [the index n in Eqs. (7), (9), (10)], 5 and 20, are used to compute similarity (Euclidean distance) of the 16 proteins selected from different CE-fold groups. Altering the order of descriptors changes the distances of proteins [e.g., the Euclidean distance of 1theB to 1o0eA is 28.74 in Fig. 7(A), which is 13.36 in Fig 7(B)]. Also, the relative distance of pairs changes, which is obvious from the different topology of the two trees [Fig. 7(A,B)]. When the order of five is used [Fig. 7(A)], an emphasis is given to describe overall shapes, such as spherical, cylinder like, or tadpole-like shapes. With the order of 20, clusters made by using the order of five are further decomposed [Fig. 7(B)]. To highlight the decomposition of clusters between the two trees, clusters of proteins within the Z -value of the Euclidean distance of 0.35 are shaded by the same color. The Z -score of the Euclidean distance using the order of 20 and 5 is computed using the average and the standard deviation of the distribution of distances of protein pairs in the CE benchmark dataset. Reducing resolution will also contribute in the search speed, because the descriptor becomes more compact. 121 numbers are used in a descriptor when the order n is set to 20, and it is decreased to 12 when the order is set to 5.

DISCUSSION

Here, we have introduced 3D Zernike descriptor as a novel computationally efficient method for searching protein tertiary structures. Unlike the other existing methods for structure comparison and representation, the 3D Zernike descriptor allows an extremely rapid database search, which opens up the possibility for a real time protein tertiary structure search on the internet. The search speed can be further increased by prescreening proteins by their length and/or by multi-resolution search using different orders of the descriptor. A search

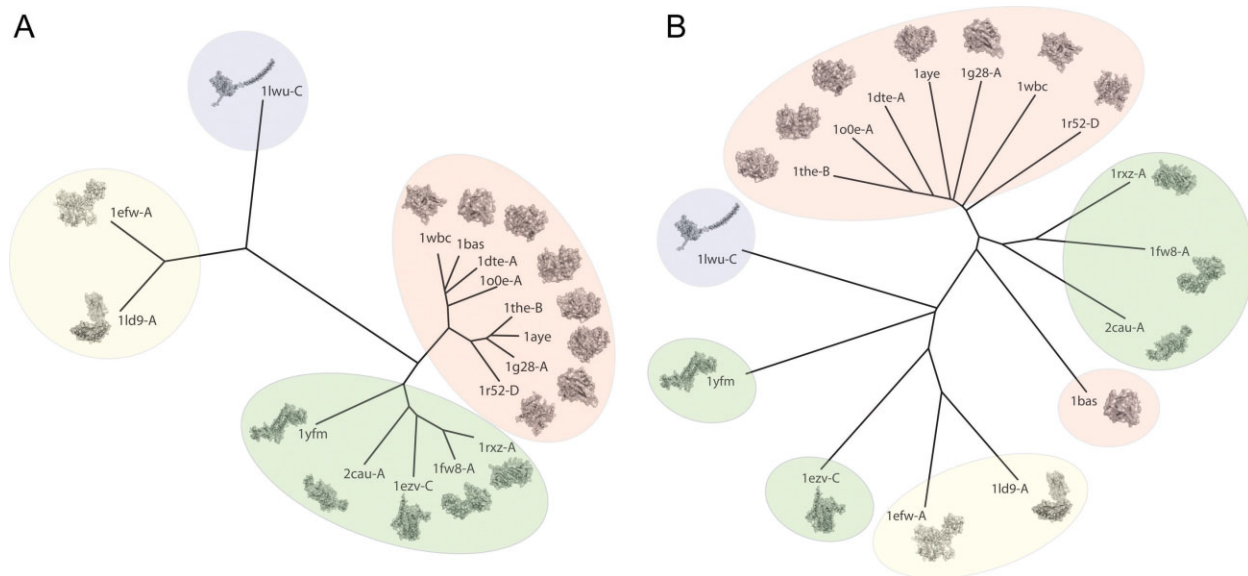


Figure 7

Resolution of 3D Zernike descriptor. **A**, 3D Zernike descriptors of the order of five; **B**, the order of 20 is used to construct trees representing similarity of the surface shape of 16 proteins: 1theB, 1o0eA, 1dteA, 1aye, 1g28A, 1wbc, 1r52D, 1rxzA, 1fw8A, 2cauA, 1bas, 1ld9A, 1efwA, 1ezvC, 1yfm, and 1lwuC. The Euclidean distance is used. Proteins within a Z-value of distance of 0.35 are grouped in a colored circle. The colors represent proteins in the same cluster in the tree constructed by using the order of five. The Z-value is calculated using the average and the standard deviation of the distribution of the Euclidean distances of proteins in the CE benchmark dataset. Phylip package⁶⁶ Fitch-Margoliash method is used to construct the trees. The length of the stems connecting two proteins represents the distance between them. The distance between 1theB to 1aye and 1theB to 1o0eA in Figure 6(A,B) is 15.95 (17.57) and 28.74 (13.36), respectively.

against the benchmark dataset of 2432 proteins used in this work took only 0.46 s. This indicates by a simple computation that a search against the current entire PDB database with 45,000 proteins would take 18.5 s. A pre-eminent mathematical property of 3D Zernike descriptor is that it is rotation invariant. This is a significant advantage over spherical harmonics and the multipole representation⁴² that need to pose structures on a reference frame for comparison.

Because 3D Zernike descriptor concerns surface shape of proteins but not main chain orientation, in principle proteins found to be similar by 3D Zernike descriptor does not necessarily have evolutionary relationship, as illustrated in Figure 5. However, our benchmark results show that in majority of the cases 3D Zernike descriptor retrieves protein structures of the same fold (Table II), thus demonstrates its utility in regular protein global structure database search. In a practical implementation of a tool for a real-time protein structure search, 3D Zernike descriptor could be used as a rapid primary filter, followed by an option to use a conventional structure comparison method, such as CE, to compute main-chain similarity between a query protein against retrieved top 10–20 structures.

Moreover, surface shape representation made possible by 3D Zernike descriptors has numerous intriguing applications. A possible application is 3D shape matching

for images by electron microscopy or electron tomography. Currently, we are developing local protein surface shape comparison and search algorithms for structure-based function annotation.⁶⁷ It would also be interesting to analyze surfaces of proteins or biological molecules with a similar function but different main-chain or molecular structure, such as binding sites of DNA-binding proteins, or proteins that display structural mimicry.⁶⁸

Biology has entered an informatics era when efficient reuse of knowledge from existing databases is crucial. In biological sequence comparison, BLAST and FASTA have enabled fast database search more than a decade ago, which revolutionized biological research. In contrast, handling of protein 3D structures is still in the realm of pairwise comparison, by which a 3D structure database search may still take hours. That would certainly render 3D structure search impractical and hinder the development of novel tools-/applications-based fast structure search. We believe that the fast real-time 3D structure search enabled by 3D Zernike descriptors, so to speak, 3D-BLAST, will lead us to a paradigm shift in research concerning protein tertiary structure.

REFERENCES

- Gutteridge A, Thornton JM. Understanding nature's catalytic toolkit. *Trends Biochem Sci* 2005;30:622–629.

2. Winter C, Henschel A, Kim WK, Schroeder M. SCOPPI: a structural classification of protein-protein interfaces. *Nucleic Acids Res* 2006;34(Database issue):D310–D314.
3. Jefferson ER, Walsh TP, Roberts TJ, Barton GJ. SNAPPI-DB: a database and API of Structures, Interfaces and Alignments for Protein-Protein Interactions. *Nucleic Acids Res* 2007;35(Database issue): D580–D589.
4. Orengo CA, Thornton JM. Protein families and their evolution—a structural perspective. *Annu Rev Biochem* 2005;74:867–900.
5. Hawkins T, Luban S, Kihara D. Enhanced automated function prediction using distantly related sequences and contextual association by PFP. *Protein Sci* 2006;15:1550–1556.
6. Hawkins T, Kihara D. Function prediction of uncharacterized proteins. *J Bioinform Comput Biol* 2007;5:1–30.
7. Hawkins T, Chitale M, Kihara D. New paradigm in protein function prediction for large scale omics analysis. *Mol Biosystems* 2008;4: 223–231.
8. Service R. Structural biology. Structural genomics, round 2. *Science* 2005;307:1554–1558.
9. Burley SK. An overview of structural genomics. *Nat Struct Biol* 2000;7 (Suppl):932–934.
10. Zhang C, Kim SH. Overview of structural genomics: from structure to function. *Curr Opin Chem Biol* 2003;7:28–32.
11. Berman HM, Westbrook J, Feng Z, Gilliland G, Bhat TN, Weissig H, Shindyalov IN, Bourne PE. The Protein Data Bank. *Nucleic Acids Res* 2000;28:235–242.
12. Altschul SF, Gish W, Miller W, Myers EW, Lipman DJ. Basic local alignment search tool. *J Mol Biol* 1990;215:403–410.
13. Pearson WR, Lipman DJ. Improved tools for biological sequence comparison. *Proc Natl Acad Sci USA* 1988;85:2444–2448.
14. Chothia C, Lesk AM. The relation between the divergence of sequence and structure in proteins. *EMBO J* 1986;5:823–826.
15. Wilson CA, Kreychman J, Gerstein M. Assessing annotation transfer for genomics: quantifying the relations between protein sequence, structure and function through traditional and probabilistic scores. *J Mol Biol* 2000;297:233–249.
16. Kinoshita K, Nakamura H. Identification of the ligand binding sites on the molecular surface of proteins. *Protein Sci* 2005;14:711–718.
17. Fetrow JS, Godzik A, Skolnick J. Functional analysis of the *Escherichia coli* genome using the sequence-to-structure-to-function paradigm: identification of proteins exhibiting the glutaredoxin/thioredoxin disulfide oxidoreductase activity. *J Mol Biol* 1998;282:703–711.
18. Torrance JW, Bartlett GJ, Porter CT, Thornton JM. Using a library of structural templates to recognise catalytic sites and explore their evolution in homologous families. *J Mol Biol* 2005;347:565–581.
19. Mizuguchi K, Go N. Seeking significance in three-dimensional protein structure comparisons. *Curr Opin Struct Biol* 1995;5:377–382.
20. Kolodny R, Petrey D, Honig B. Protein structure comparison: implications for the nature of 'fold space', and structure and function prediction. *Curr Opin Struct Biol* 2006;16:393–398.
21. Kabsch W. A discussion of the solution for the best rotation to relate two sets of vectors. *Acta Crystallogr* 1978;A34827–A34828.
22. Kihara D, Skolnick J. The PDB is a covering set of small protein structures. *J Mol Biol* 2003;334:793–802.
23. Shindyalov IN, Bourne PE. Protein structure alignment by incremental combinatorial extension (CE) of the optimal path. *Protein Eng* 1998;11:739–747.
24. Gerstein M, Levitt M. Using iterative dynamic programming to obtain accurate pairwise and multiple alignments of protein structures. *Proc Int Conf Intell Syst Mol Biol* 1996;459–467.
25. Orengo CA, Taylor WR. SSAP: sequential structure alignment program for protein structure comparison. *Methods Enzymol* 1996; 266:617–635.
26. Holm L, Sander C. Protein structure comparison by alignment of distance matrices. *J Mol Biol* 1993;233:123–138.
27. Zhou X, Chou J, Wong ST. Protein structure similarity from principle component correlation analysis. *BMC Bioinformatics* 2006;7:40.
28. Mizuguchi K, Go N. Comparison of spatial arrangements of secondary structural elements in proteins. *Protein Eng* 1995;8:353–362.
29. Vogel C, Morea V. Duplication, divergence and formation of novel protein topologies. *Bioessays* 2006;28:973–978.
30. Zhang Y, Skolnick J. The protein structure prediction problem could be solved using the current PDB library. *Proc Natl Acad Sci USA* 2005;102:1029–1034.
31. Via A, Ferre F, Brannetti B, Helmer-Citterich M. Protein surface similarities: a survey of methods to describe and compare protein surfaces. *Cell Mol Life Sci* 2000;57:1970–1977.
32. Dupuis F, Sadoc JF, Jullien R, Angelov B, Mornon JP. Voro3D: 3D Voronoi tessellations applied to protein structures. *Bioinformatics* 2005;21:1715–1716.
33. Connolly ML. Solvent-accessible surfaces of proteins and nucleic acids. *Science* 1983;221:709–713.
34. Edelsbrunner H, Mücke EP. 3-Dimensional α -shapes. *Acm Trans Graphics* 1994;13:43–72.
35. Macke TJ, Duncan BS, Goodsell DS, Olson AJ. Interactive modeling of supramolecular assemblies. *J Mol Graph Model* 1998;16:115–113.
36. Novotni M, Klein R. 3D Zernike descriptors for content based shape retrieval. ACM symposium on solid and physical modeling proceedings of the 8th ACM symposium on Solid modeling and applications 2003;216–225.
37. Orengo CA, Michie AD, Jones S, Jones DT, Swindells MB, Thornton JM. CATH—a hierarchic classification of protein domain structures. *Structure* 1997;5:1093–1108.
38. Lo Conte L, Brenner SE, Hubbard TJ, Chothia C, Murzin AG. SCOP database in 2002: refinements accommodate structural genomics. *Nucleic Acids Res* 2002;30:264–267.
39. Holm L, Sander C. Touring protein fold space with Dali/FSSP. *Nucleic Acids Res* 1998;26:316–319.
40. Madej T, Gibrat JF, Bryant SH. Threading a database of protein cores. *Proteins* 1995;23:356–369.
41. Kinoshita K, Nakamura H. Identification of protein biochemical functions by similarity search using the molecular surface database eF-site. *Protein Sci* 2003;12:1589–1595.
42. Gramada A, Bourne PE. Multipolar representation of protein structure. *BMC Bioinformatics* 2006;7:242.
43. Morris RJ, Najmanovich RJ, Kahraman A, Thornton JM. Real spherical harmonic expansion coefficients as 3D shape descriptors for protein binding pocket and ligand comparisons. *Bioinformatics* 2005;21:2347–2355.
44. Kazhdan M, Chazelle B, Dobkin D, Funkhouser T, Rusinkiewicz S. A reflective symmetry descriptor for 3D models. *Algorithmica* 2004;38:201–225.
45. Dym H, McKean H. Fourier series and integrals. New York: Academic Press; 1972.
46. Kazhdan M, Funkhouser T, Rusinkiewicz S. Rotation invariant spherical harmonic representation of 3D shape descriptors. Proceedings of the 2003 Eurographics/ACM SIGGRAPH symposium on Geometry processing 2003;43156–43164.
47. Funkhouser T, Min P, Kazhdan M, Chen J, Halderman A, Dobkin D, Jacobs D. A search engine for 3D models. *Acm Trans Graphics* 2003;22:83–105.
48. Hu M-K. Visual pattern recognition by moment invariants. *IRE Trans Inf Theory* 1962;8:179–187.
49. Hu M-K. Pattern recognition by moment invariants. *Proc IRE* 1961;49:1428.
50. Sheng Y, Arsenault HH. Experiments on pattern-recognition using invariant Fourier-Mellin descriptors. *J Opt Soc Am A: Opt Image Sci Vis* 1986;3:771–776.
51. Casasent D, Psaltis D. Scale invariant optical transform. *Opt Eng* 1976;15:258–261.
52. Teh CH, Chin RT. On image-analysis by the methods of moments. *IEEE Trans Pattern Anal Machine Intelligence* 1988;10:496–513.

53. Foon NH, Pang Y-H, Jin ATB, Ling DNC. Efficient Method for Human Face Recognition Using Wavelet Transform and Zernike Moments. Proc Int Conf Comp Graphics, Imaging and Visualization (CGIV'04) 2004;0065–0069.
54. Asadi MR, Vahedi A, Amindavar H. Leukemia cell recognition with Zernike moments of holographic images. Signal Processing Symposium 2006 NORSIG 2006 Proceedings of the 7th Nordic 2006;214–217.
55. Bayraktar B, Banada PP, Hirleman ED, Bhunia AK, Robinson JP, Rajwa B. Feature extraction from light-scatter patterns of *Listeria* colonies for identification and classification. J Biomed Opt 2006;11:34006.
56. Yeh JS, Chen DY, Chen BY, Ouhyoung M. A web-based three-dimensional protein retrieval system by matching visual similarity. Bioinformatics 2005;21:3056–3057.
57. Canterakis N. 3D Zernike moments and Zernike affine invariants for 3D image analysis and recognition. Proceedings of the 11th Scandinavian Conference on Image Analysis 1999;85–93.
58. Laga H, Takahashi H, Nakajima M. Spherical wavelet descriptors for content-based 3D model retrieval. IEEE international conference on shape modeling and applications 2006 (SMF'06). IEIC Tech Rep 2006;105:49–54.
59. Connolly ML. Shape complementarity at the hemoglobin alpha 1 beta 1 subunit interface. Biopolymers 1986;25:1229–1247.
60. Kriegel H-P, Kroger P, Mashaël Z, Pfeifle M, Potke M, Seidl S. Effective similarity search on voxelized CAD objects. Proceedings of 8th international conference on database systems for advanced applications 2003;27–36.
61. Jiantao P, Ramani K. A 3D model retrieval method using 2d free-hand sketches. International conference on computational science 2005;343–346.
62. Jayanti S, Kalyanaraman Y, Iyer N, Ramani K. Developing an engineering shape benchmark for CAD models. Comput-Aided Des 2006;38:939–953.
63. Holm L, Park J. DaliLite workbench for protein structure comparison. Bioinformatics 2000;16:566–567.
64. Godzik A. The structural alignment between two proteins: is there a unique answer? Protein Sci 1996;5:1325–1338.
65. Sierk ML, Pearson WR. Sensitivity and selectivity in protein structure comparison. Protein Sci 2004;13:773–785.
66. Felsenstein J. PHYLIP—Phylogeny Inference Package (Version 3.2). Cladistics 2005;5164–5166.
67. Li B, Turuvekere S, Agrawal M, La D, Ramani K, Kihara D. Characterization of local geometry of protein surfaces with the visibility criterion. Proteins 2008;71:670–683.
68. Stebbins CE, Galan JE. Structural mimicry in bacterial virulence. Nature 2001;412:701–705.